Available online at www.sciencedirect.com

ScienceDirect

International Journal of Solids and Structures 44 (2007) 5182–5207

INTERNATIONAL JOURNAL OF SOLIDS and STRUCTURES

www.elsevier.com/locate/ijsolstr

Functionally graded structural members obtained via the low temperature strain induced phase transformation

B. Skoczeń *

Institute of Applied Mechanics, Faculty of Mechanical Engineering, Cracow University of Technology, Al. Jana Pawła II 37, Cracow, Poland

Received 9 September 2006; received in revised form 18 November 2006
Available online 29 December 2006

Abstract

The notion of functionally graded materials (FGM) covers all domains of discrete and smooth gradation of material microstructure designed in order to obtain macroscopic features suitable for a given application. A special class of multi-phase materials with graded microstructure can be obtained at cryogenic temperatures as a result of smooth transition from the parent phase to the secondary phase. The required continuously graded material features are obtained at low temperatures via the mechanism of controlled strain induced phase transformation from the purely austenitic to the martensitic lattice ($\gamma \rightarrow \alpha'$). Several families of ductile materials are known to behave in a metastable way when strained at very low temperatures. Among them the austenitic stainless steels are extensively used to construct components of the superconducting magnets, cryogenic transfer lines and other structural members loaded in cryogenic conditions. The constitutive model used to describe mathematically the plastic strain induced phase transformation at low temperatures involves strain hardening where two fundamental effects play an important role: interaction of dislocations with the martensite inclusions and increase in material tangent stiffness due to the mixture of harder martensite with softer austenite. The interaction of dislocations with the martensite inclusions is reflected by the hardening modulus that depends on the volume fraction of martensite. Here, a linear approximation, based on the micro-mechanics analysis, is used. On the other hand, evaluation of the material tangent stiffness of two-phase continuum is based on the classical homogenization scheme and takes into account the local tangent moduli of the components, as postulated by Hill [Hill, R., 1965. A self consistent mechanics of composite materials. J. Mech. Phys. Solids 13, 213–222]. In the present paper, the Mori–Tanaka homogenisation scheme is applied. Both effects contribute to strong nonlinear hardening that occurs as soon as the phase transformation process begins. The material model is suitable for a wide range of temperatures, however the best results are obtained at very low temperatures, where the linearized kinetic law of phase transformation is valid [Garion, C., Skoczeń B., 2002. Modeling of plastic strain induced martensitic transformation for cryogenic applications. J. Appl. Mech. 69 (6), 755–762]. As the application field the structural members in the form of rods (cylinders) of circular cross-section, used as parts of the carrying structures, are analyzed. The required graded microstructure of the material is obtained by imposing torsion at cryogenic temperatures. Both the intensity of the phase transformation and the depth of the transformed zone is obtained by suitable kinematic control (angle of twist). The closed form solutions for the stress state and torque as a function of the angle of twist are shown.

Keywords: FGM, functionally graded materials; Cryogenic temperatures; Phase transformation; Torsion

* Tel.: +48 12 628 33 84; fax: +48 12 648 45 31.
E-mail addresses: blazej.skoczen@pk.edu.pl, blazej.skoczen@cern.ch

0020-7683/$ - see front matter
doi:10.1016/j.ijsolstr.2006.12.032

1. Introduction

The concept of functionally graded materials was initiated and technologically developed in Japan (Koizumi, 1992, 1997; Koizumi and Niino, 1995). Initially the effort was focused on development of thermally resistant materials, in particular thermal barriers. Gradually, the notion of functionally graded materials covered all domains of discrete and smooth gradation of material structure in order to obtain macroscopic features necessary for a given application. The natural domains of application of the FGMs are the components confronted with extreme temperatures in the aerospace industry, nuclear power plants, plasma containing devices, fission and fusion reactors as well as the cryogenic installations including the superconducting magnets.

The attractive feature of the graded materials consists in the fact that the mathematically optimized material microstructure can be manufactured by using sophisticated technologies that are now industrially available. Typical processing techniques used to obtain a graded microstructure are (cf. Kieback et al., 2003): powder metallurgy, melt processing and processing of polymers. The manufacturing processes consist usually of two stages: the process of constructing the graded material structure from the precursor components called "gradation" and the process of final aggregation of the bulk material called "consolidation". Typical consolidation processes are sintering or solidification. The fundamental technological issues related to the production of FGMs are the composition of powder, particle size and shape, packing density, porosity, grain size, etc.

As soon as the material microstructure is defined the problem of mathematical description arises. Standard RVE approach to the description of highly inhomogeneous graded materials is based on the homogenization techniques. The idea of homogenization postulates replacing a heterogeneous portion of the material, contained in the representative volume element (RVE), by a quasi-homogeneous portion, response of which is determined from a suitable averaging procedure. The well known homogenization schemes for two-phase continuum are the rule of mixtures, the self-consistent scheme (Hershey, 1954; Kröner, 1958; Hill, 1965) as well as the Mori–Tanaka scheme (Mori and Tanaka, 1973). The homogenization schemes perform correctly under the assumption that the elastic inclusions embedded into the elastic matrix can be regarded as ellipsoidal or spherical in shape (Eshelby, 1957). The bounds on the equivalent moduli of the isotropic heterogeneous materials were defined by Paul, 1960 and later by Hashin and Shtrikman, 1963. Here, the variational bounding techniques of linear elasticity were used to obtain the estimates of the elastic moduli. The predictions of homogenization models have been thoroughly compared with the experimental data and finite element analysis by Pierard et al., 2004. The authors took into account the following schemes for two-phase isothermal composites: Voigt and Reuss models, Mori–Tanaka model with the interpretation by Benveniste (1987), double-inclusion model and the self-consistent scheme. In addition the homogenization of multi-phase isothermal composites has been reviewed. An exact method of homogenization of an unbounded finitely deformed solid containing the ellipsoidal inclusions, based on the generalized Eshelby tensor, has been developed by Nemat-Nasser (1999, 2000). Another useful RVE based technique is the periodic homogenization combined with two-scale asymptotic expansion method (cf. Alzina et al., 2006). All above mentioned techniques assume building a mesoscopic representative volume element that is applied as an elementary brick to construct the macroscopic response of the material. Such approach may face serious limitations in the case of fast evolution of material properties or large field gradients developed in the material. It may generate high modeling errors especially in the case of strong localization of strains and stresses. An improved, higher order theory taking into account the micro-macrostructural coupling effect has been developed by Pindera and Dunn (1997) and Aboudi et al. (1999). The approach is based on volumetric averaging of field quantities and imposition of boundary and interfacial conditions between the sub-volumes defined within the FGM. An extension of the model including the inelastic behaviour of constituent phases of multiphase periodic materials has been recently proposed by Aboudi et al., 2003. The problem of homogenization of rate-independent elastic–plastic composites (cf. Doghri and Ouaar, 2003) has been already solved by Hill, 1965, who linearized the constitutive equations and defined the local elastic–plastic tangent moduli. Based on these moduli a classical homogenization scheme (for instance the self consistent model) can be applied at every load step. Thus, the elastic–plastic analysis consists in performing a sequence of homogenization operations on the step-by-step basis, including the constantly evolving tangent moduli for all components of the composite. A similar approach has been applied by Garion and Skoczeń (2002), to the elastic–plastic matrix containing elastic inclusions, with the application of the Mori–Tanaka scheme. Finally, the macroscopic response of two-phase elastic–viscoplastic composites

has been computed by using the improved affine formulation by Pierard and Doghri (2006). The elastic–visco-plastic constitutive equations of each phase were linearized to obtain fictitious linear thermo-elastic relations and the classical homogenization schemes were again applied. The authors indicate good performance of the Mori–Tanaka scheme for the composite materials, confirmed by a comparison with the finite element analysis.

1.1. Axisymmetric elastic structural components made of functionally graded materials

Among different structural members a special class of problems constitute the axisymmetric components like disks, cylinders and cylindrical shells made of functionally graded materials. The rotationally symmetric geometry is on one hand very convenient from the point of view of mathematical description and – on the other hand – particularly useful in the technical applications. Stationary thermo-elastic analysis of functionally graded anisotropic cylinders subjected to temperature gradients and mechanical loads (tension, torsion, shear and pressure load) has been carried out by Tarn (2001). Exact solutions for the temperature distribution, stress and strain fields for inhomogeneous hollow and solid cylinders were presented by the author. The thermo-elastic material moduli were assumed to vary as power functions of the cylinder radius. For more complex functions representing the variation of material moduli a model based on a multilayer representation has been suggested. The state space formalism to solve the problem of cylinders composed of n anisotropic layers subjected to torsion and bending has been developed by Tarn and Wang (2001). The cases of generalized plane strain and generalized torsion were thoroughly analyzed. The solution was presented separately for the axisymmetric state (axial tension, torsion, pressure and shear) as well as for the asymmetric case of bending. The authors found interaction between the solutions corresponding to axial tension, torsion and pressure. Another attempt to solve the B. de Saint-Venant problem comprising tension, bending and flexure of functionally graded cylinders made of elastic isotropic material with the elastic moduli varying across the cross-section was presented by Rooney and Ferrari (2001). The lower bounds on the effective elastic moduli were derived. The authors indicate that the elastic moduli are convex functions of the volume fractions. Moreover, the authors demonstrate that if the structural member is subjected to bending then concentrating the phases with higher Young's modulus away from the neutral axis reduces the deformation under a given bending moment. Another class of problems related to axisymmetric structures made of functionally graded materials emerges from the stability analysis. Sofiyev and Schnack (2004), studied stability of functionally graded thin shells subjected to torsional loading varying as a linear function of time. For the effective material properties the rule of mixtures was applied. The volume fractions of the constituents were assumed to follow a simple power law. The authors obtained analytical solutions for the dynamic critical torsional loads.

1.2. Axisymmetric elastic–plastic structural components made of non-homogeneous materials

Numerous papers are dedicated to elastic–plastic response of axisymmetric components (bars of circular cross-section, cylinders, disks, circular plates and cylindrical shells) made of homogeneous materials. However, the problem becomes much more complicated when the material non-homogeneity is assumed. Analysis of non-homogeneous thick-walled cylinders under inner pressure and axial load was carried out by Olszak and Urbanowski (1955). Another problem of non-homogeneous elastic–plastic orthotropic circular plates subjected to bending was analyzed by Olszak and Murzewski (1957). Limit analysis and design of transversally non-homogeneous axially symmetric shells was dealt with by Olszak and Sawczuk (1957). The equations of general axisymmetric case in thick-walled tubes including the circularly symmetric plastic non-homogeneity (yield stress being an arbitrary function of the radius) have been formulated by Życzkowski (1957a). The author indicates that in some particular cases of plastic non-homogeneity, when the yield stress is inversely proportional to the square of the radius or to the fourth power of radius, the solution for stresses reduces from the hyper-elliptic to elliptic integrals. In the same year the limit states of the non-homogeneous rotating discs were analyzed by Życzkowski (1957b). A theory of plastic-rigid solid reinforced by inextensible fibers was developed by Smith and Spencer (1970). In the framework of this theory the authors analyzed plastic deformations of thick-walled cylinders reinforced by helical inextensible fibers. A random distributed non-homogeneity of the material, combined with associated and non-associated flow rules, and applied to the limit analysis of structures has been developed by Sacchi (1971). The problem of plastic torsion of non-homogeneous prismatic

bars, both in the general case of transversal non-homogeneity and in the particular case when the yield stress is a quadratic function of the radius, has been investigated by Życzkowski (1981). For the particular case the closed form solutions were obtained and the limit carrying capacity of the cross-section has been determined. It is worth pointing out, that already in the eighties Życzkowski introduced an idea of optimum material non-homogeneity leading to the effect of uniform and simultaneous plastification at failure of the whole cross-section. This idea can certainly be regarded as a precursor of the optimum functional distribution of the material properties. Following this proposal two papers dealing with the problem of full plastification of circular non-homogeneous cylinders were published by Kordas and Wróblewski (1987), as well as by Kordas and Dollar (1990).

More recently analytical solutions for thermal stresses in the cylindrical joints made of functionally graded materials were presented by Yang (2000). Both the elastic and the creep behavior of the material were analyzed. The author assumed that the creep response of the material is represented by the Norton's law. For the creep problem the asymptotic solution was shown. Finally, it is worth highlighting the recent effort to obtain an optimum layout of volume fractions in a functionally graded material. A methodology of multi-objective optimization of volume fraction distribution for two-phase functionally graded materials subjected to temperature fields and heat fluxes has been developed by Goupee and Vel (2006). The effective material properties were estimated by using the Mori–Tanaka and the self consistent homogenization schemes. The effective yield stress for the metal–metal functionally graded materials was determined by using the Hashin–Shtrikman bounds. For the optimization process the multi-objective genetic algorithms were used. The design objectives were formulated either as minimum mass + minimum of the peak effective stress or as minimum mass + maximum of the safety factor. The authors indicate that the methodology is well suited for determining the Pareto-optimum solutions when designing the material composition of functionally graded materials.

2. Functionally graded materials applied at cryogenic temperatures

A special class of multi-phase materials with graded microstructure can be obtained as a result of smooth transition from the parent phase to the secondary phase. The required continuously graded material features are obtained at low temperatures via the mechanism of controlled strain induced phase transformation from the purely austenitic lattice (face cubic centred – FCC) to the martensitic lattice (body cubic centred – BCC). Several families of ductile materials are known to behave in a metastable way when cooled down or strained at very low temperatures. Among them the austenitic stainless steels are extensively used to construct pressure and vacuum vessels, components of the superconducting magnets, components of the cryogenic transfer lines and other structural members loaded in cryogenic conditions. Metastable ductile materials may undergo either spontaneous phase transformation or strain induced transformation. The stainless steels commonly used for low temperature applications (like 304L, 316L or 316LN) have the chemical structure tailored to eliminate the spontaneous phase transformation. On the other hand, in the case of plastic straining at low temperatures the strain induced martensitic transformation is inevitable and leads to creation of a two-phase heterogeneous continuum where the initial austenitic γ-phase has been locally replaced by the α' martensite inclusions. The BCC lattice of the martensite inclusions is much harder when compared to the FCC austenitic lattice and affects considerably the material behaviour. This feature is used to obtain a material with graded strength function.

Another specific class of materials with the continuously graded microstructure form the so-called magnetically graded materials (Watanabe and Sakai, 2003) obtained again by the $\gamma \rightarrow \alpha'$ phase transformation techniques. A smooth distribution of the magnetisation function across the specimen is characteristic of this class of materials. As the γ phase is paramagnetic and the α' phase is ferromagnetic, the increase in martensite fraction promoted by plastic deformation can be detected by measuring the magnetic permeability μ. The results of local measurements can be stored in order to obtain a profile of the magnetisation along the sample. However, it is necessary to control simultaneously the temperature and the strain distribution during the technological process.

Some of the FGMs applied at low temperatures are known to have a discretely graded microstructure. Such a heterogeneous microstructure is well represented by the family of modern superconductors with a programmed redistribution of the flux pinning centres. Type II superconductors are characterised by the existence

of the so-called mixed state, which allows the magnetic flux to penetrate the material. The flux forms an array of individual flux lines (so-called fluxon lattice), which can be pinned against imperfections and inclusions (Van Sciver, 1986). Flux pinning allows the superconductor to carry high currents in the magnetic fields close to the upper critical field H_{c2}. Type II superconductors with the controlled redistribution of the flux pinning centres can be classified as the FGMs with discretely graded microstructure.

Important class of functionally graded materials for low and ultra-low temperature applications comprises thin films and coatings. Thin films are typically applied as the superconducting layers in the radio-frequency accelerating cavities of the particle accelerators (Benvenuti et al., 1984, 1993). Here, the copper cavities coated with a thin superconducting niobium film were successfully applied. Typical technology consists in 1.5-μm thick niobium films grown by magnetron sputtering in argon atmosphere on oxidised copper substrates. The superconducting niobium films operate at 4.2 K in liquid helium. Other superconducting materials such as: NbTi, NbTiN or Nb_3Sn, can also be used.

Another family of materials applied at low temperatures constitute graded coatings in the form of getters and non-evaporable getters (NEG). They are used either in the form of graded strips or thin-film coatings. These active materials provide the so-called linear distributed pumping (absorption of the residual molecular gas) that allows extremely low pressures down to 10^{-14} mbar to be achieved under the static vacuum conditions. Typical application the NEG materials find in the long vacuum chambers (made of copper or aluminium) of the superconducting particle accelerators. The most common alloys used as the activated getters are ZrAl, ZrVFe as well as TiZrV (Benvenuti et al., 2001). Thin films of getter material are coated on the inner surface of the vacuum chambers by sputtering technology. Together with the base material of the vacuum chamber they form graded layers characterised by smoothly evolving density and porosity.

One of the possible application fields both at low and at higher temperatures are structural members in the form of rods (cylinders) of circular cross section, used as parts of the carrying structures. The required graded structure of the material is obtained by imposing torsion at cryogenic temperatures. Both the intensity of the phase transformation and the depth of the transformed zone is obtained by suitable kinematic control (angle of twist). In the present paper, the constitutive model of $\gamma \to \alpha'$ plastic strain induced phase transformation and its application to torsion at cryogenic temperatures are presented. The closed form solutions for the stress state and torque as a function of the angle of twist are shown.

3. Plastic strain induced ($\gamma \to \alpha'$) phase transformation at cryogenic temperatures

3.1. Kinetics of phase transformation and related phenomena

The plastic strain induced $\gamma \to \alpha'$ phase transformation in metastable materials like stainless steels occurs in a wide range of temperatures. For instance, it can be easily activated at 77 K, in liquid nitrogen. The process is controlled via the transformation kinetics, represented by the phase transformation curve. Kinetics of $\gamma \to \alpha'$ phase transformation, developed by Olson and Cohen (1975), is reflected by a typical sigmoidal curve defining the evolution of the martensite content (ξ) as a function of the plastic strain. Under isothermal conditions and for a given strain rate, the classical sigmoidal curve has the form shown in Fig. 1. At very low temperatures the phase transformation process can be subdivided into three stages: low rate transformation below the threshold p_ξ (stage I), fast transformation with a high and nearly constant transformation rate (stage II) and asymptotically vanishing transformation with the rate decreasing to 0 and the volume fraction of martensite reaching a maximum ξ_L (stage III).

Constitutive modeling of the plastic strain induced $\gamma \to \alpha'$ phase transformation has already a long history. A constitutive equation predicting the stress as a function of strain, strain rate and temperature for metastable austenites has been derived by Narutani et al. (1982). The contributions of two major factors controlling the flow stress: static hardening and dynamic softening were separated. The transformation strain corrected rule of mixtures was used to describe the static hardening. The dynamic softening was derived by treating the martensitic transformation as a deformation mechanism. The quantitative description of both contributions to the flow behaviour led to the constitutive model for which the knowledge of the transformation curves and the flow properties of both phases was needed. Another constitutive model developed by Stringfellow et al. (1992), for nonthermoelastic alloys introduced a generalized version of the Olson–Cohen transformation

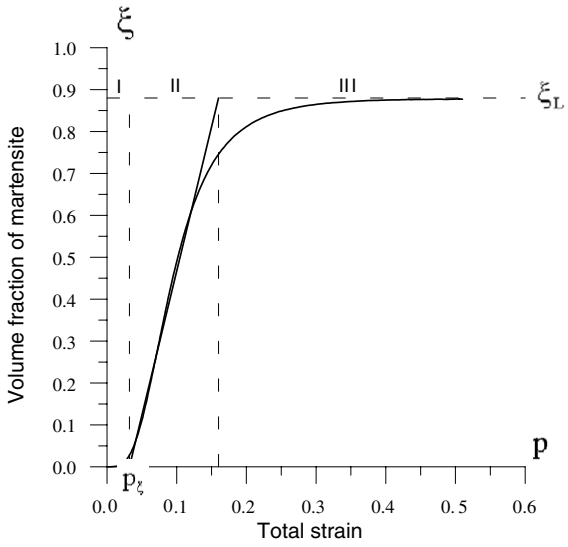

Fig. 1. Volume fraction of martensite versus accumulated plastic strain.

kinetics, where the evolution of martensite was a function of temperature, plastic strain and the stress state. The authors assumed that the transformation process generates a nucleation strain that can be decomposed into the deviatoric and hydrostatic components. Isotropic hypoelastic formulation was applied to describe the stress state evolution. The strain softening resulting from the transformation strain was incorporated into the model. The self consistent approach describing the deviatoric plastic strain rate has been applied. The Eshelby solutions for isotropic, incompressible spherical inclusions embedded in an infinitely extended incompressible isotropic matrix were used as a basis for the localization law. The law has been extended to the case of nonlinear viscous materials, for which the deformation within the inclusion was no longer uniform.

Another approach, based on microplasticity coupled with the phase transformation was proposed by Fischer et al. (1998). The formulation was based on the conditional extremum problem. The dissipation inequality under the yield and transformation constraints constitutes the core of the formulation. Full coupling between the phase transformation and plasticity has been taken into account in the constitutive equations. A specific form of the Gibbs potential as well as the yield and transformation conditions have been presented. A quantitative prediction of the volume fraction of martensite in austenitic stainless steel under thermo-mechanical loading was derived by Diani and Parks (1998). The basic assumption of the Olson–Cohen model has been adopted for each grain in the material. The authors assumed that the nucleation sites of the α' martensite within a grain are localized at the intersection of shear bands. Motion of dislocations on the slip systems characteristic of the γ austenite was analyzed. Further analysis was performed already on a polycrystalline aggregate. The shear intensity defined the evolution of volume fraction of martensite in each grain. The model was checked on grade 304L stainless steel, typical of the low temperature applications. A mesoscopic continuum thermo-mechanical approach applied to the strain induced martensitic transformation was developed by Levitas et al. (1999). Finite plastic and transformation strains and small elastic deformations were taken into account. The model was based on the multiplicative decomposition of the total deformation gradient into elastic, transformation and plastic parts. The generalized Prandtl-Reuss equations for isotropic elasto-plastic materials, including large plastic and transformation strains, were applied. Transformation criterion and extremum principle for determination of location and volume of transformed domains were formulated. A revised formulation of the transformation induced plasticity has been presented by Fischer et al. (2000). Both the influence of transformation induced plastic strain and the influence of shear (orientation effect) on the irreversible deformation were taken into account. A new constitutive description for the elasto-plastic materials subjected to the phase transformation has been developed. A micromechanical analysis of the internal stress sources, resulting either from the incompatible transformation strain accompanying the phase transformation or from the plastic flow of both phases due to the motion of dislocations has been developed by

Cherkaoui et al. (2000). According to the authors the main complexity in the modeling of the behaviour of TRIP steels consists in evaluation of the effect of internal stresses on the $\gamma \rightarrow \alpha'$ phase transformation. A microscale mechanism of the martensitic phase transformation was taken into account. Formation of martensite microdomains with moving boundaries inside inhomogeneous plastic strain fields was assumed. Coherent interfaces with discontinuities of stress and strain fields across the multiple moving boundaries were introduced. As a potential describing the thermodynamic state of the two-phase system the Helmholtz free energy was chosen. The morphology of microdomains was represented by the ellipsoidal inclusions with one dimension much smaller when compared to the other two dimensions. The Eshelby description of an inelastic ellipsoidal inclusion was applied. A suitable kinetics of the martensitic transformation was developed. The constitutive model was applied to an austenitic single crystal. In order to make a transition to the polycrystalline TRIP steels an elasto-plastic self consistent algorithm was used.

A new and broader constitutive description including the effect of strain rate, temperature as well as the applied stress has been presented by Tomita and Iwamoto (2001). The model was tested on grade 304 austenitic stainless steel and for the temperature range 77–353 K. The phase transformation (evolution of martensite) has been described as a function of temperature, prestrain, applied stress as well as the stress range. Numerical tests on steel bars with ringed notches under cyclic loads were performed. A general formulation of the finite thermoplasticity model including the phase transformation has been presented by Dachowski and Boehm (2004). The model is based on the concept of isomorphism of elastic ranges. The evolution of different phases is described in terms of the mass fractions, treated as the internal variables. As the model is general, it can be used to describe different types of thermo-mechanical processes where the phase transformation takes place. A microstructure based computational model has been developed by Han et al. (2004). Again the shear band intersections were assumed as the locations of the martensite nucleation sites. The activation of the nucleation sites was function of the interaction energy between the stress state and the lattice deformation. A self-consistent approach was applied to describe the deformation behaviour of each material phase. The uniaxial tension and simple shear were used as the test cases for comparison between the experiments and the numerical simulation. Another constitutive model has been recently developed by Iwamoto (2004), who focused on deformation behaviour of TRIP steel with growth of martensite sites due to the phase transformation. The effect of the geometrical configuration of martensite sites on the macroscopic behaviour of TRIP steels was investigated. Growth of ellipsoidal martensitic inclusion embedded in the austenitic matrix has been analyzed using a homogenization technique. The author assumed that the mechanical properties of TRIP steels can be enhanced due to controlled geometrical characteristics of the martensite fraction in the austenitic matrix. In the model the transformation-thermo-coupled asymptotic homogenization was applied. The model included the transformation strain rate and latent heat induced by the phase transformation.

3.2. Formulation of the constitutive model

If the plastic strain induced phase transformation occurs at very low temperatures (typically liquid helium 4.2 K or liquid nitrogen 77 K) then the steep part of the transformation curve (Fig. 1, stage II) remains in the domain of relatively small strains (below 0.2). In this case the constitutive modeling can be considerably simplified and stays within the scope of the classical rate independent theory of plasticity. A simplified evolution law for the volume fraction of martensite has been introduced for the linear part (II) of the sigmoidal curve by Garion and Skoczeń (2002)

$$\dot{\xi} = A(T, \underline{\underline{\dot{\varepsilon}}}^{\mathrm{p}}, \underline{\underline{\sigma}})\dot{p}H((p - p_{\xi})(\xi_{\mathrm{L}} - \xi)) \tag{1}$$

where $\dot{p}$ denotes the rate of the accumulated plastic strain, defined as

$$\dot{p} = \sqrt{\frac{2}{3}\underline{\underline{\dot{\varepsilon}}}^{\mathrm{p}} : \underline{\underline{\dot{\varepsilon}}}^{\mathrm{p}}} \tag{2}$$

Here, ξ denotes the volume fraction of martensite, $A(..)$ is a function of temperature, stress state (Stringfellow et al., 1992) and strain rate (Levitas et al., 1999), p_{ξ} denotes the accumulated plastic strain threshold (to trigger the formation of martensite), ξ_{L} stands for the martensite content limit and H represents the Heaviside func-

tion. The phase transformation from the FCC to BCC lattice is driven by the accumulated plastic strain obtained by monotonic or cyclic straining at low temperatures.

The constitutive model applied in the present paper describes behaviour of a ductile material in which the phase transformation occurs. The model is based on the following assumptions:

- two-phase continuum consists of the austenitic matrix and martensite platelets represented by small Eshelby type ellipsoidal inclusions randomly distributed and randomly oriented in the matrix,
- the austenitic matrix is assumed elasto-plastic, whereas the inclusions show purely elastic response (the yield stress of martensite fraction is much higher than the yield stress of austenite),
- rate independent plasticity is applied: it is assumed that the influence of the strain rate $\dot{\underline{\underline{\varepsilon}}}^{p}$ is small for the range of temperatures 2–77 K (cf. Hecker et al., 1982) and function $A(..)$ depends on the temperature and stress state only,
- small strains are assumed: the accumulated plastic strain p does not exceed 0.2,
- mixed isotropic/kinematic hardening affected by the presence of martensite fraction is included,
- the two-phase material obeys the associated flow rule.

It is worth pointing out that even if the current model is valid under the assumption of small strains, there is no fundamental difficulty to extend the model for large strains. The limitation of the accumulated plastic strain to 0.2 has a meaning for monotonic loads, whereas for cyclic loads the limitation should rather be imposed on maximum strains on cycle and not on the accumulated plastic strain (the Odqvist parameter), that may substantially increase from cycle to cycle. A generalization of the model to large strains leads inevitably to the application of different strain measure (for instance the Hencky measure). However, it is worth stressing that the current model yields correct results (as shown in the course of the paper) even for the values of the accumulated plastic strain exceeding 0.2, in the case of monotonic loading.

Another important problem is related to the shape of martensite inclusions. The ellipsoidal Eshelby type representation has the feature of being general enough to cover different shapes of martensite variant. Indeed, by choosing the appropriate parameters a flat platelet can be easily obtained. However, if the phase transformation process is not massive and much less than 50% of the parent volume is consumed by the new phase, even a spherical representation is reasonable as the average distance between the inclusions is large enough and the effect of mutual interaction of the strain fields produced by the neighbouring inclusions becomes less important. In such a case, both the self consistency method and the Mori–Tanaka homogenization scheme can be applied.

The following set of constitutive equations has been developed for the two-phase ($\gamma + \alpha'$) isotropic and ductile material (Garion and Skoczeń, 2002).

The kinetics of martensitic transformation takes the form

$$\dot{\xi} = A(T, \underline{\underline{\sigma}})\dot{p}H((p - p_{\xi})(\xi_{L} - \xi)) \tag{3}$$

The general constitutive law includes plastic, thermal and transformation strains

$$\underline{\underline{\sigma}} = \underline{\underline{\underline{\underline{E}}}} : (\underline{\underline{\varepsilon}} - \underline{\underline{\varepsilon}}^{p} - \underline{\underline{\varepsilon}}^{th} - \xi\underline{\underline{\varepsilon}}^{bs}) \tag{4}$$

where $\underline{\underline{\varepsilon}}^{p}$ is the plastic strain tensor, $\underline{\underline{\varepsilon}}^{bs} = \frac{1}{3}\Delta v\underline{\underline{I}}$ denotes the free deformation called bain strain, expressed in terms of the relative volume change Δv, $\underline{\underline{\varepsilon}}^{th}$ stands for the thermal strain tensor and $\underline{\underline{\underline{\underline{E}}}}$ is the fourth-rank elasticity tensor. It is assumed that the mesoscopic strain tensor $\underline{\underline{\varepsilon}}^{bs}$ is obtained by integrating the microscopic eigen-strain tensor $\underline{\underline{\varepsilon}}_{\mu}^{bs}$ over the RVE

$$\underline{\underline{\varepsilon}}^{bs} = \frac{1}{V}\int_{V} \underline{\underline{\varepsilon}}_{\mu}^{bs}\,dV \tag{5}$$

The above integral can be presented in the following way:

$$\underline{\underline{\varepsilon}}^{bs} = \frac{V_{\gamma}}{V}\frac{1}{V_{\gamma}}\int_{V_{\gamma}} \underline{\underline{\varepsilon}}_{\mu}^{bs}\,dV + \frac{V_{\alpha}}{V}\frac{1}{V_{\alpha}}\int_{V_{\alpha}} \underline{\underline{\varepsilon}}_{\mu}^{bs}\,dV \tag{6}$$

where V_γ, V_α denote the volume occupied by the austenite and the volume occupied by the martensite in the RVE, respectively. Assuming that the microscopic eigen-strain in the austenitic phase is equal to zero

$$\underline{\underline{\varepsilon}}^{\mathrm{bs}}_{\mu} = \underline{\underline{0}} \tag{7}$$

one obtains the following equation:

$$\underline{\underline{\varepsilon}}^{\mathrm{bs}} = \frac{V_\alpha}{V}\frac{1}{V_\alpha}\int_{V_\alpha}\underline{\underline{\varepsilon}}^{\mathrm{bs}}_{\mu}\,\mathrm{d}V = \xi\frac{1}{V_\alpha}\int_{V_\alpha}\underline{\underline{\varepsilon}}^{\mathrm{bs}}_{\mu}\,\mathrm{d}V = \xi\langle\underline{\underline{\varepsilon}}^{\mathrm{bs}}_{\mu}\rangle \tag{8}$$

where $\langle\underline{\underline{\varepsilon}}^{\mathrm{bs}}_{\mu}\rangle$ denotes the average (over the RVE) of eigen-strain in the martensitic phase. In the case of displacive transformation the eigen-strain tensor takes the following form (Wechsler et al., 1953; Fischer, 1997):

$$\underline{\underline{\varepsilon}}^{\mathrm{bs}}_{\mu} = \begin{pmatrix} 0 & 0 & \frac{\gamma}{2} \\ 0 & 0 & 0 \\ \frac{\gamma}{2} & 0 & \Delta v \end{pmatrix}_{(\vec{x},\vec{y},\vec{z})} \tag{9}$$

where $\vec{x},\vec{y},\vec{z}$ stands for the local coordinate system. The habit plane of the martensite variant is represented by $(\vec{x},\vec{y})$, whereas $\vec{z}$ is the normal vector. The transformation shear is denoted by γ and the volume change by Δv. Owing to the fact that the orientation of martensite platelets is determined with respect to the orientation of the grains, that are randomly oriented in the initial austenitic structure, one can expect a random orientation of martensite inclusions in the RVE. Therefore, by integrating the microscopic eigen-strain over the RVE one obtains a purely isotropic tensor

$$\left\langle\underline{\underline{\varepsilon}}^{\mathrm{bs}}_{\mu}\right\rangle = \frac{1}{3}\Delta v\underline{\underline{I}} \tag{10}$$

Finally, the mesoscopic free strain tensor is equal to

$$\underline{\underline{\varepsilon}}^{\mathrm{bs}} = \xi\frac{1}{3}\Delta v\underline{\underline{I}} \tag{11}$$

For convenience of description it is assumed that the elastic stiffness tensor is expressed by

$$\underline{\underline{\underline{\underline{E}}}} = 3k\underline{\underline{\underline{\underline{J}}}} + 2\mu\underline{\underline{\underline{\underline{K}}}} \tag{12}$$

where tensors $\underline{\underline{\underline{\underline{J}}}}, \underline{\underline{\underline{\underline{K}}}}$, are volumetric and deviatoric 4th rank projectors, respectively

$$\underline{\underline{\underline{\underline{J}}}} = \frac{1}{3}\underline{\underline{I}}\otimes\underline{\underline{I}} \quad ; \quad \underline{\underline{\underline{\underline{K}}}} = \underline{\underline{\underline{\underline{I}}}} - \underline{\underline{\underline{\underline{J}}}} \tag{13}$$

In the standard notation one obtains:

$$J_{ijkl} = \frac{1}{3}\delta_{ij}\delta_{kl}; \quad I_{ijkl} = \frac{1}{2}(\delta_{ik}\delta_{jl} + \delta_{il}\delta_{jk}) \tag{14}$$

Here, symbol $\otimes$ denotes the dyadic product, δ_{ij} is the Kronecker symbol and k, μ denote the bulk and the shear moduli, respectively.

As the model is based on the rate independent plasticity, the yield surface has the form

$$f_y\left(\underline{\underline{\sigma}}, \underline{\underline{X}}, R\right) = J_2(\underline{\underline{\sigma}} - \underline{\underline{X}}) - \sigma_y - R \tag{15}$$

where

$$J_2(\underline{\underline{\sigma}} - \underline{\underline{X}}) = \sqrt{\frac{3}{2}(\underline{\underline{s}} - \underline{\underline{X}}) : (\underline{\underline{s}} - \underline{\underline{X}})} \tag{16}$$

is the second invariant of the stress tensor. Here, $\underline{\underline{s}}, \underline{\underline{X}}$ denote the deviatoric stress and the back stress tensors, whereas σ_y, R are the yield stress and the isotropic hardening variable, respectively. In the current approach it is assumed that the quasi-isotropic two-phase continuum obeys the associated flow rule

$$\mathrm{d}\underline{\underline{\varepsilon}}^{\mathrm{p}} = \frac{\partial f_y}{\partial \underline{\underline{\sigma}}}\,\mathrm{d}\lambda \tag{17}$$

with the yield function postulated as the potential of plasticity. The hardening model is represented by the following equations:

$$\dot{\underline{\underline{X}}} = \frac{2}{3} C_X \dot{\underline{\underline{\varepsilon}}}^{\mathrm{p}} = \frac{2}{3} g(\xi) \dot{\underline{\underline{\varepsilon}}}^{\mathrm{p}} \tag{18}$$

$$\dot{R} = C_R \dot{p} = f(\xi)\dot{p} \tag{19}$$

Since the hardening variables R and $\underline{\underline{X}}$ are affected by the presence of martensite, the corresponding evolution laws are postulated in the following incremental form:

$$\mathrm{d}\underline{\underline{X}} = \mathrm{d}\underline{\underline{X}}_a + \mathrm{d}\underline{\underline{X}}_{a+m} = \frac{2}{3} C(\xi)\mathrm{d}\underline{\underline{\varepsilon}}^{\mathrm{p}} + G(\xi)\mathrm{d}\underline{\underline{\varepsilon}}^{\mathrm{p}} = \frac{2}{3} g(\xi)\mathrm{d}\varepsilon^{\mathrm{p}} \tag{20}$$

$$\mathrm{d}R = f(\xi)\,\mathrm{d}p \tag{21}$$

It is assumed that the back stress increment is composed of the classical term which corresponds to the behavior of the austenitic phase $\mathrm{d}\underline{\underline{X}}_a$ in the presence of localized small inclusions, uniformly distributed and randomly oriented in the RVE and a term related to the combination of austenite and martensite via the homogenization algorithm ($\mathrm{d}\underline{\underline{X}}_{a+m}$). Furthermore, it is assumed that the mechanism of plastic flow at low temperatures is based on the motion of dislocations in the lattice. If the massive motion of dislocations occurs they are stopped by the martensite inclusions and the corresponding local stress fields (Fig. 2).

The principal components that constitute the two-phase material model are the elasto-plastic matrix (austenite) and the highly localized elastic inclusions (martensite platelets). Linear kinematic hardening law is applied to model the plastic behavior of the pure austenite

$$\mathrm{d}\underline{\underline{X}}_{a0} = \frac{2}{3} C_0\,\mathrm{d}\underline{\underline{\varepsilon}}^{\mathrm{p}} \tag{22}$$

where C_0 is the hardening modulus of the original non-transformed purely austenitic phase. For the two-phase transformed material, the hardening modulus C_0 is replaced by the modulus C, that is higher than C_0 because of the interactions between the dislocations in the austenite and the martensite inclusions

$$C = C_0\varphi(\xi) \quad \text{for } 0 \leqslant \xi \leqslant \xi_{\mathrm{L}};\ \varphi(0) = 1 \tag{23}$$

It can be easily shown that the shear stress necessary for a dislocation to pass across two inclusions of the average size d, separated by the distance l, depends roughly linearly on the volume fraction of martensite ξ

$$\tau_p = \frac{\mu b}{d}\left(\frac{6\xi_0}{\pi}\right)^{\frac{1}{3}}\left(1 + \frac{\xi - \xi_0}{3\xi_0}\right) \tag{24}$$

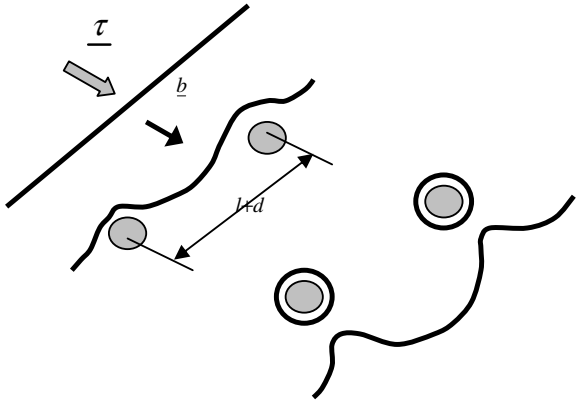

Fig. 2. Interaction between dislocation and inclusions – the Orowan mechanism.

where μ denotes the shear modulus of the austenite, b is the length of the Burgers vector and ξ_0 stands for the initial volume fraction of inclusions. Here, for the sake of simplicity, an assumption has been made that the average size of inclusions (d) is constant and much smaller than the distance between two inclusions ($d \ll l$). In the light of Eq. (24), the function $\varphi(\xi)$ takes the linear form

$$\varphi(\xi) = h\xi + 1 \tag{25}$$

where h is a material dependent parameter. The function $\varphi(\xi)$ can be interpreted as this part of the hardening process that corresponds to the increase in volume fraction of martensite and enhanced probability that a dislocation will stack on an inclusion. The back stress increment corresponding to the behavior of austenite in the presence of highly localized martensite inclusions can be decomposed in the following way:

$$\mathrm{d}\underline{\underline{X}}_a = \mathrm{d}\underline{\underline{X}}_{a0} + \mathrm{d}\underline{\underline{X}}_{a\xi} = \frac{2}{3}C_0\,\mathrm{d}\underline{\underline{\varepsilon}}^{\mathrm{p}} + \frac{2}{3}C_0 h\xi\,\mathrm{d}\underline{\underline{\varepsilon}}^{\mathrm{p}} = \frac{2}{3}C(\xi)\mathrm{d}\underline{\underline{\varepsilon}}^{\mathrm{p}} \tag{26}$$

where $\mathrm{d}\underline{\underline{X}}_{a\xi}$ corresponds to the interactions between the dislocations in the austenitic matrix and the martensite inclusions.

The second contribution to the hardening model is based on the principle of homogenization applied on the step-by-step basis to the current linearized tangent stiffness moduli of the matrix and the inclusions (Fig. 3). As the matrix (γ-phase) is elastic–plastic, the relevant local linearized tangent stiffness tensor is derived. The inclusions are assumed to be ellipsoidal in shape and elastic (Eshelby, 1957), therefore, the elastic tangent stiffness is applied. The process of step-by-step homogenization based on the local tangent stiffness moduli follows the concept introduced by Hill (1965).

For the pure austenitic phase, a linearization of the stress/strain relations in the vicinity of the current state is expressed by

$$\Delta\underline{\underline{\sigma}}_a = \underline{\underline{\underline{\underline{E}}}}_t : \Delta\underline{\underline{\varepsilon}} \tag{27}$$

where $\underline{\underline{\underline{\underline{E}}}}_t$ is the tangent stiffness tensor. A similar principle can be applied to the two-phase continuum. However, the tangent stiffness tensor is obtained by the homogenization process

$$\Delta\underline{\underline{\sigma}}_{a+m} = \underline{\underline{\underline{\underline{E}}}}_H : \Delta\underline{\underline{\varepsilon}} \tag{28}$$

The additional hardening increment induced by the presence of the martensite is given by

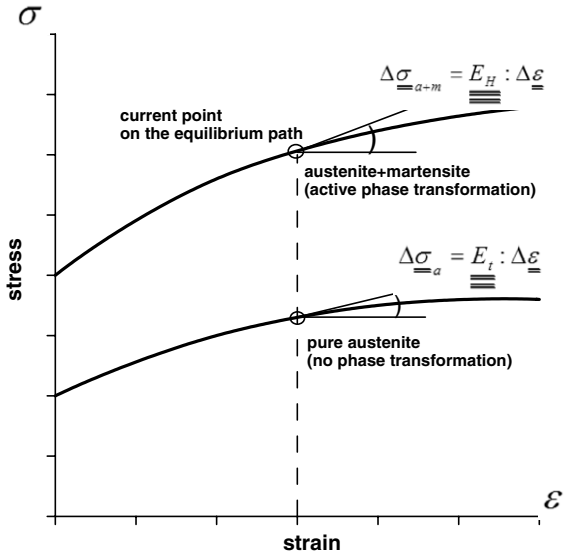

Fig. 3. The principle of homogenization based on the local tangent stiffness moduli.

$$\Delta\underline{\underline{\sigma}} = \Delta\underline{\underline{\sigma}}_{a+m} - \Delta\underline{\underline{\sigma}}_{a} = \left(\underline{\underline{\underline{\underline{E}}}}_{H} - \underline{\underline{\underline{\underline{E}}}}_{t}\right) : \Delta\underline{\underline{\varepsilon}} \tag{29}$$

Here, the same "trial" strain increment has been assumed for pure austenite and for the homogenized two-phase continuum in order to compute the macroscopic stress response in the case of strain controlled process. In the next chapters mainly kinematically controlled $\gamma \rightarrow \alpha'$ phase transformation processes will be analyzed. The local linearized stiffness of the austenite can be described by the following tangent stiffness tensor:

$$\underline{\underline{\underline{\underline{E}}}}_{ta} = 3k_{ta}\underline{\underline{\underline{J}}} + 2\mu_{ta}\underline{\underline{\underline{K}}} \tag{30}$$

where

$$\mu_{ta} = \frac{E_t}{2(1+\nu)}; \quad k_{ta} = \frac{E_t}{3(1-2\nu)}; \quad E_t = \frac{EC}{E+C} \tag{31}$$

As the tangent operator for plastically active processes contains a dyadic square product of the vector normal to the yield surface in the stress space which makes the operator anisotropic, a linearization based on the quasi-isotropic operator is particularly justified in the case when the absolute values of the principal stresses are close to each other. When compared to the matrix the inclusions are isotropic and elastic (their yield point is much higher than for the pure austenite) and the corresponding elastic stiffness tensor is given by:

$$\underline{\underline{\underline{\underline{E}}}}_{m} = 3k_{m}\underline{\underline{\underline{J}}} + 2\mu_{m}\underline{\underline{\underline{K}}} \tag{32}$$

where

$$\mu_{m} = \frac{E}{2(1+\nu)}; \quad k_{m} = \frac{E}{3(1-2\nu)} \tag{33}$$

The inclusions are assumed ellipsoidal and uniformly distributed in the matrix. Application of the Mori–Tanaka homogenization scheme yields

$$\underline{\underline{\underline{\underline{E}}}}_{H} = \underline{\underline{\underline{\underline{E}}}}_{\mathrm{MT}} = 3k_{\mathrm{MT}}\underline{\underline{\underline{J}}} + 2\mu_{\mathrm{MT}}\underline{\underline{\underline{K}}} \tag{34}$$

with $\underline{\underline{\underline{\underline{E}}}}_{\mathrm{MT}}$ obtained from the following relation:

$$\left[\underline{\underline{\underline{\underline{E}}}}_{\mathrm{MT}} + \underline{\underline{\underline{\underline{E}}}}^{*}\right]^{-1} = \sum_{i=a,m} f_i \left[\underline{\underline{\underline{\underline{E}}}}_{i} + \underline{\underline{\underline{\underline{E}}}}^{*}\right]^{-1} \tag{35}$$

where f_i is the volume fraction of the component "i" and $\underline{\underline{\underline{\underline{E}}}}^{*}$ stands for the Hill influence tensor. After some rearrangements the following equations are obtained:

$$\begin{aligned} 3k_{\mathrm{MT}} + 3k^{*} &= \left[\frac{1-\xi}{3(k_{ta}+k^{*})} + \frac{\xi}{3(k_{m}+k^{*})}\right]^{-1} \\ 2\mu_{\mathrm{MT}} + 2\mu^{*} &= \left[\frac{1-\xi}{2(\mu_{ta}+\mu^{*})} + \frac{\xi}{2(\mu_{m}+\mu^{*})}\right]^{-1} \\ k^{*} &= \frac{4}{3}\mu_{ta}; \quad 2\mu^{*} = \frac{\mu_{ta}(9k_{ta}+8\mu_{ta})}{3(k_{ta}+2\mu_{ta})} \end{aligned} \tag{36}$$

As the strain increment is mainly due to the plastic strains: $\Delta\,\underline{\underline{\varepsilon}} \cong \Delta\underline{\underline{\varepsilon}}^{\mathrm{p}}$, Eq. (29) becomes

$$\Delta\underline{\underline{\sigma}} = \left(\underline{\underline{\underline{\underline{E}}}}_{MT} - \underline{\underline{\underline{\underline{E}}}}_{t}\right) : \Delta\underline{\underline{\varepsilon}}^{\mathrm{p}} \tag{37}$$

The plastic strains are represented by a deviatoric tensor, therefore

$$\underline{\underline{\underline{\underline{J}}}} : \Delta\underline{\underline{\varepsilon}}^{\mathrm{p}} = \underline{\underline{0}}; \quad \underline{\underline{\underline{\underline{K}}}} : \Delta\underline{\underline{\varepsilon}}^{\mathrm{p}} = \Delta\underline{\underline{\varepsilon}}^{\mathrm{p}} \tag{38}$$

Finally, the additional stress increment due to the presence of martensite in the austenitic matrix is equal to

$$\Delta\underline{\underline{\sigma}} = 2(\mu_{\mathrm{MT}} - \mu_{ta})\Delta\underline{\underline{\varepsilon}}^{\mathrm{p}} \tag{39}$$

If pure kinematic hardening is considered, the evolution of the back stress for two-phase continuum obeys the following equation:

$$\Delta\underline{\underline{X}}_{a+m} = \Delta\underline{\underline{\sigma}} \tag{40}$$

or in the incremental form

$$\mathrm{d}\underline{\underline{X}}_{a+m} = 2(\mu_{\mathrm{MT}} - \mu_{ta})\,\mathrm{d}\underline{\underline{\varepsilon}}^{\mathrm{p}} \tag{41}$$

On the other hand, if pure isotropic hardening is considered, the evolution of the hardening parameter is obtained by imposing the suitable norm on the stress tensor:

$$\Delta R = \Delta R_{a+m} = \|\Delta\underline{\underline{\sigma}}\| = \sqrt{\Delta\underline{\underline{\sigma}} : \Delta\underline{\underline{\sigma}}} = 2(\mu_{\mathrm{MT}} - \mu_{ta})\Delta p \tag{42}$$

where $\Delta p = \sqrt{\frac{2}{3}\Delta\underline{\underline{\varepsilon}}^{\mathrm{p}} : \Delta\underline{\underline{\varepsilon}}^{\mathrm{p}}}$. In the incremental form one obtains:

$$\mathrm{d}R = \mathrm{d}R_{a+m} = 2(\mu_{\mathrm{MT}} - \mu_{ta})\,\mathrm{d}p \tag{43}$$

Thus, for a unidirectional process of monotonic loading the stress increments corresponding to the same increment of plastic strain are identical both for the kinematic hardening and for the isotropic hardening models. This linearized approach to the evolution of isotropic hardening is replaced by a more general nonlinear formulation, suitable for higher martensite content:

$$\mathrm{d}R = (R_{\infty}(\xi) - R)\mathrm{d}p \tag{44}$$

where R_{∞} is the parameter that defines the ultimate size of the yield surface:

$$R_{\infty}(\xi) = 2(\mu_{\mathrm{MT}} - \mu_{ta}) \tag{45}$$

Eq. (44) can be reduced to Eq. (43) in the vicinity of the initial state.

In order to establish a proportion between the kinematic and the isotropic hardening the Baushinger parameter β is introduced (parametrization after Życzkowski, 1981):

$$\beta = \frac{\sigma' + \sigma'^{-}}{2(\sigma' - \sigma_0)}; \quad 0 \leqslant \beta \leqslant 1 \tag{46}$$

where (σ') denotes the stress level at unloading and (σ'^{-}) is the stress level corresponding to the reverse active process. The parameter varies between 0 for the isotropic hardening (no Bauschinger effect) and 1 for the kinematic hardening (perfect Bauschinger effect).

Finally, the mixed hardening is described by the following model:

$$\mathrm{d}\underline{\underline{X}} = \frac{2}{3}C_X\,\mathrm{d}\underline{\underline{\varepsilon}}^{\mathrm{p}} = \frac{2}{3}[C(\xi) + 3\beta b(\xi)(\mu_{\mathrm{MT}} - \mu_{ta})]\mathrm{d}\underline{\underline{\varepsilon}}^{\mathrm{p}} \tag{47}$$

$$\mathrm{d}R = C_R\mathrm{d}p = b(\xi)(1-\beta)(R_{\infty}(\xi) - R)\mathrm{d}p \tag{48}$$

The relaxation term $b(\xi) = 1 - \xi$ has been added in order to compensate for the assumption that the martensite inclusions are elastic, whereas – in reality – they behave in elastic–plastic way. The process of phase transformation induced strain hardening stops when $\xi = 1$.

The above presented mixed hardening model has the following advantages:

1. the model involves both the mesoscopic and the macroscopic levels,
2. the principal constituents of the two-phase material model are the elasto-plastic matrix (austenite) and the elastic inclusions (martensite platelets),

3. the evolution of back stress is partially driven by the interaction between the dislocations and the martensite sites dispersed in the austenitic matrix (the approach justified by microscopic considerations),
4. the evolution of back stress depends significantly on the properties and amount of both fractions via the Mori–Tanaka homogenization,
5. the Mori–Tanaka homogenization is performed by using the tangent stiffness of both constituents (austenite and martensite) obtained via the linearization in the vicinity of the current state (cf. Hill, 1965),
6. the isotropic hardening parameter tends asymptotically to the value determined by the ultimate size of the yield surface,
7. the ultimate size of yield surface is a function of the properties and amount of both fractions (γ, α') via the Mori–Tanaka homogenization.
8. proportion between the kinematic and the isotropic hardening is defined by the Bauschinger parameter.

It is worth pointing out that the model is attractive in view of its simplicity and relatively small number of parameters to be identified at cryogenic temperatures. The experiments carried out in liquid helium or nitrogen are laborious, expensive and usually require complex cryogenic installations to maintain stable conditions (constant temperature). Therefore, any justified simplification leading to reduction of the number of parameters to be determined is of great importance.

3.3. Experimental validation of the constitutive model

In order to validate the model (cf. Garion and Skoczeń, 2002), it has been confronted with the experimental results obtained by Morris et al. (1992) on 304L samples tested at 77 K under tensile monotonic loading (Fig. 4). Identification of the material parameters was based on two curves: stress versus strain (tensile test) and volume fraction of martensite versus plastic strain. The first curve has been obtained from a simple tensile test at 77 K. Simultaneously, the magnetic permeability of the sample has been measured under a predefined magnetic field. A correlation between the volume fraction of martensite (α' phase is ferromagnetic) and the magnetic permeability of the sample provides the necessary information for construction of the second curve: volume fraction of martensite versus plastic strain. The numerical simulation has been terminated just after having reached the strain level 0.2, which in this particular case corresponds approximately to the martensite content saturation level (end of region II). Typical set of material data, characteristic of grade 304L stainless steel, needed for the numerical analysis, is shown in Table 1.

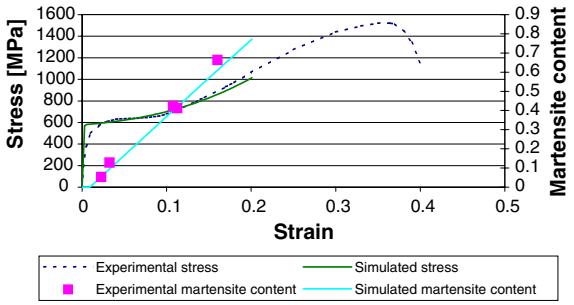

Fig. 4. Stress and martensite content versus strain for the grade 304L stainless steel at 77 K.

Table 1
Set of data for grade 304L stainless steel at 77 K (*based on Suzuki et al., 1988)

E (GPa)	ν	σ_y (MPa)	C_0 (MPa)	h	A	p_ξ	$\breve{\xi}_L$	β*	Δv
190	0.3	580	750	1.9	4.23	0.004	0.9	0.45	0.05

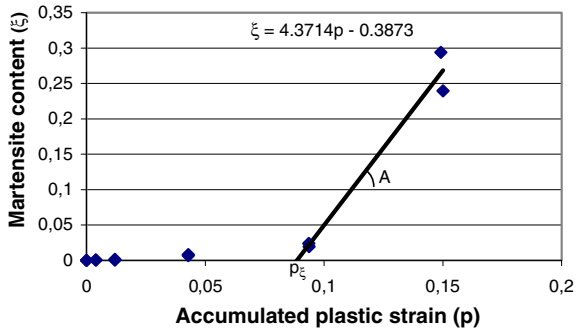

Fig. 5. Identification of parameters for grade 316L stainless steel at 77 K.

Table 2
Parameters of phase transformation identified for grade 316L at three temperature levels

Temperature	p_ξ	A
RT	0.39	0.023
77 K	0.09	4.37
4.2 K	0.08	5.1

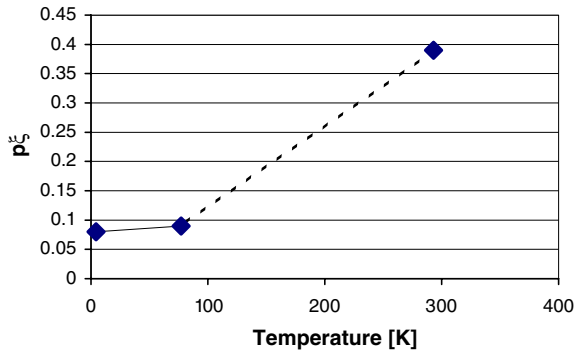

Fig. 6. Phase transformation threshold (p_ξ) as a function of temperature.

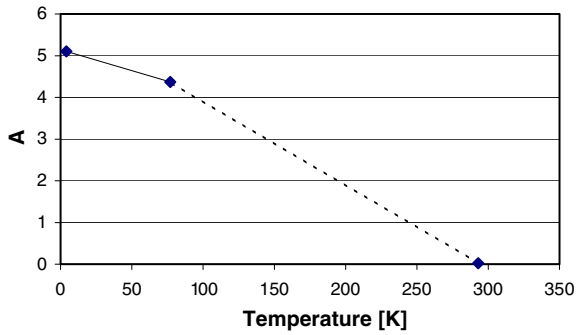

Fig. 7. Slope (A) of the martensitic transformation as a function of temperature.

Another example of experimental validation consists in identification of the parameters for grade 316L stainless steel at three temperature levels (RT, 77 K, 4.2 K). Typical evolution of martensite content as a function of accumulated plastic strain at 77 K is shown in Fig. 5.

Table 3
Set of material parameters identified for grade 316L stainless steel at 77 K

E (GPa)	ν	σ_y (MPa)	C_0 (MPa)	h	A	p_ξ	Δv
206	0.3	630	1680	2.7	4.37	0.09	0.05

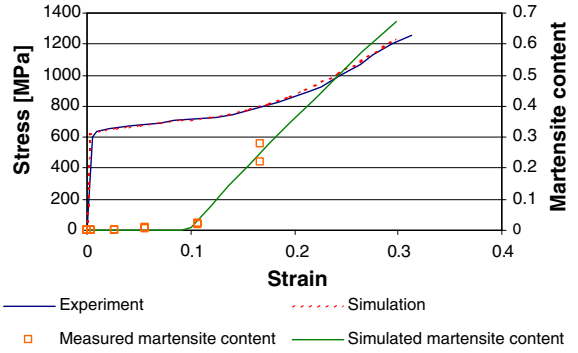

Fig. 8. Simulated stress–strain curve for grade 316L stainless steel compared with the experimental curve obtained at 77 K.

The evolution of two fundamental parameters: the phase transformation threshold p_ξ and the slope A, as a function of temperature, is presented in Table 2 and illustrated in Figs. 6 and 7.

An example of stress–strain curve obtained for grade 316L at 77 K (cf. Garion et al., 2006) and compared with the curve computed from the previously identified set of material parameters (presented in Table 3) is shown in Fig. 8. C_0 has been identified in the range, where the martensitic transformation is low ($p < 0.1$). Parameter h has been identified as the best fit between the experiment and the numerical simulation.

4. Phase transformation induced by elastic–plastic torsion at low temperatures

Consider the case of pure shear represented by the non-zero component of the strain tensor:

$$\varepsilon_{23} = \frac{\gamma_{23}}{2} \tag{49}$$

where $\gamma_{23} = \gamma$ is the angle of shear. The shear strain is accompanied by the shear stress:

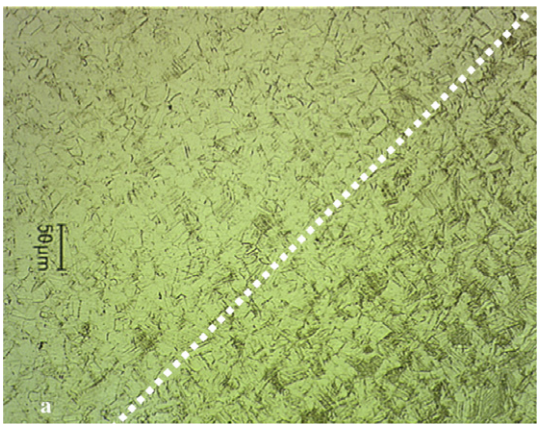

Fig. 9. Example of graded microstructure: 316L, strain 6.5%, $T = 4.2$ K, martensite concentrated below the white boundary (cf. Garion et al., 2006).

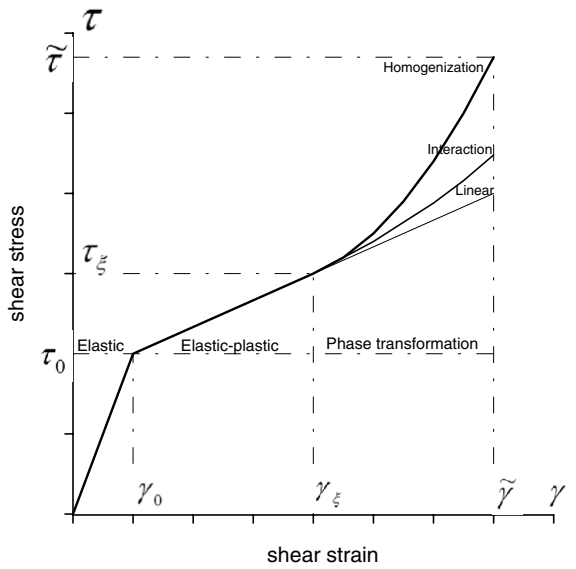

Fig. 10. Three domains of physical behaviour of the two-phase continuum.

$$\tau_{23} = \tau \tag{50}$$

Thus, the pair of variables γ, τ represents the strain and the stress in the case of pure torsion. Given the possible three domains of physical behaviour of the material, illustrated in Fig. 10, the following constitutive model is applied:

$$\tau = G\gamma; \quad \gamma < \gamma_0 \tag{51}$$

$$\tau = \tau_0 + C_0(\gamma - \gamma_0); \quad \gamma_0 \leqslant \gamma < \gamma_\xi \tag{52}$$

$$\mathrm{d}\tau = \mathrm{d}\tau_{lin} + \mathrm{d}\tau_{int} + \mathrm{d}\tau_{\mathrm{MT}} \tag{53}$$

$$\mathrm{d}\tau_{\mathrm{lin}} = C_0\,\mathrm{d}\gamma \tag{54}$$

$$\mathrm{d}\tau_{\mathrm{int}} = C_0 h\xi\,\mathrm{d}\gamma \tag{55}$$

$$\mathrm{d}\tau_{\mathrm{MT}} = C_{\mathrm{MT}}\,\mathrm{d}\gamma \tag{56}$$

where $G = \mu_{\mathrm{a}}$ denotes the shear modulus of pure austenite (elastic domain), C_0 is the basic linear hardening modulus of pure austenite and $C_0 h\xi$ is the hardening modulus of two-phase continuum, related to the interaction between the dislocations and the martensite inclusions. Here, C_{MT} stands for the hardening modulus that reflects the stiffness of the continuum containing combined austenitic and martensitic phases and γ_0, γ_ξ are the plastic and the phase transformation thresholds, respectively.

Thus, the stress increment during the phase transformation process reads:

$$\mathrm{d}\tau = C_0(1 + h\xi)\,\mathrm{d}\gamma + C_{\mathrm{MT}}\,\mathrm{d}\gamma; \quad \gamma \geqslant \gamma_\xi \tag{57}$$

Expressing the general kinetic law of phase transformation (Eq. (1)) in terms of the shear strain one derives:

$$\mathrm{d}\xi = A(T)\,\mathrm{d}\gamma^{\mathrm{p}} H[(\gamma - \gamma_\xi)(\xi_{\mathrm{L}} - \xi)] \tag{58}$$

where γ^{p} is the shear plastic strain. Assuming an isothermal process for which $A(T) = const$ and integrating Eq. (58) one obtains:

$$\xi(\tilde{\gamma}) = \int_{\gamma_\xi}^{\tilde{\gamma}} A(T)\,\mathrm{d}\gamma = A(T)(\tilde{\gamma} - \gamma_\xi) \tag{59}$$

The above formula corresponds to the linearized part II of the sigmoidal curve as shown in Figs. 1 and 11.

Inserting Eq. (59) into Eq. (57) leads to the following formula for the stress increment:

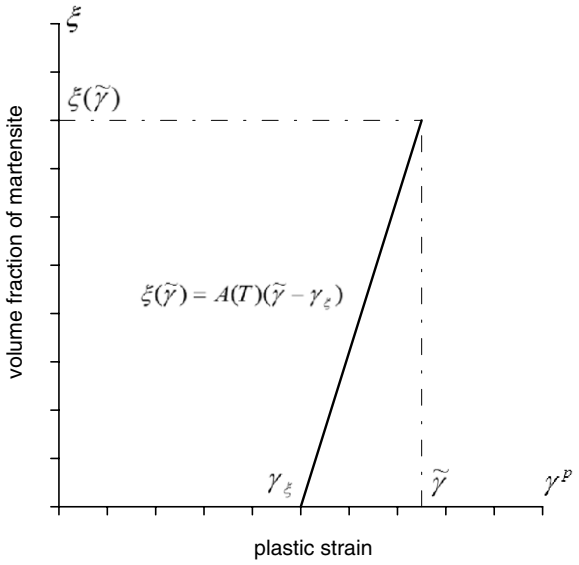

Fig. 11. Volume fraction of martensite as a function of the shear strain.

$$\mathrm{d}\tau = C_0[1 + hA(T)(\gamma - \gamma_\xi)]\,\mathrm{d}\gamma + C_{\mathrm{MT}}\,\mathrm{d}\gamma = \mathrm{d}\tau^{\mathrm{p}1} + \mathrm{d}\tau^{\mathrm{p}2}; \quad \gamma \geqslant \gamma_\xi \tag{60}$$

Integration of $\mathrm{d}\tau^{\mathrm{p}1}$ over the range $(\gamma_\xi, \tilde{\gamma})$ yields the following total stress increment:

$$\Delta\tau^{\mathrm{p}1}(\tilde{\gamma}) = \int_{\gamma_\xi}^{\tilde{\gamma}} C_0[1 + hA(T)(\gamma - \gamma_\xi)]\,\mathrm{d}\gamma = C_0\left[\Delta\gamma + \frac{h}{2}A(T)(\Delta\gamma)^2\right] \tag{61}$$

where:

$$\Delta\gamma = \tilde{\gamma} - \gamma_\xi \tag{62}$$

The second portion $\mathrm{d}\tau^{\mathrm{p}2}$ of the total stress increment is related to the Mori–Tanaka homogenization. The general equations were presented in the previous chapter. For the austenite the following tangent moduli are defined:

$$\mu_{ta} = \frac{E_t}{2(1+\nu)}; \quad E_t = \frac{EC(\xi)}{E + C(\xi)} \tag{63}$$

where $E, C(\xi)$ are the Young modulus (identical for austenite and martensite) and the current hardening modulus. The shear modulus for the martensite inclusions is expressed by:

$$\mu_m = \mu = \frac{E}{2(1+\nu)} = G \tag{64}$$

Following Eq. (39) in its incremental form, the stress increment related to the Mori–Tanaka homogenization is equal to:

$$\mathrm{d}\tau^{\mathrm{p}2} = (\mu_{\mathrm{MT}} - \mu_{ta})\,\mathrm{d}\gamma^{\mathrm{p}} = C_{\mathrm{MT}}\,\mathrm{d}\gamma^{\mathrm{p}} \tag{65}$$

Assuming for the plastic strains the incompressibility one obtains:

$$C_{\mathrm{MT}} = \frac{5}{2}\frac{\mu\eta}{1+\eta}\frac{\xi}{\left(1+\frac{5}{2}\eta\right) - \xi} \tag{66}$$

where:

$$\eta = \frac{C_0(1 + h\xi)}{E} \tag{67}$$

Making the following additional assumptions:

$$\eta \ll 1; \quad 1+\eta \approx 1; \quad 1+\frac{5}{2}\eta \approx 1 \tag{68}$$

which is justified by the hardening parameter being two orders of magnitude smaller when compared to the Young modulus. This simplification leads to the following conclusion:

$$C_{\mathrm{MT}} = \frac{5}{2}\mu\eta_0 \frac{(1+h\xi)\xi}{1-\xi} \tag{69}$$

where:

$$\eta_0 = \frac{C_0}{E} \tag{70}$$

Developing Eq. (69) in Taylor series with respect to ξ one obtains:

$$C_{\mathrm{MT}} = \frac{5}{2}\mu\eta_0[\xi + (1+h)\xi^2 + (1+h)\xi^3] \tag{71}$$

Integration of $d\tau^{\mathrm{p}2}$ over the range $(\gamma_\xi, \tilde{\gamma})$ yields the following formula for stress increment:

$$\Delta\tau^{\mathrm{p}2}(\tilde{\gamma}) = \int_{\gamma_\xi}^{\tilde{\gamma}} C_{\mathrm{MT}}(\xi)\,\mathrm{d}\gamma^{\mathrm{p}} = \frac{5}{2}G\eta_0\left[A(T)\frac{(\Delta\gamma)^2}{2} + (1+h)A^2(T)\frac{(\Delta\gamma)^3}{3} + (1+h)A^3(T)\frac{(\Delta\gamma)^4}{4}\right] \tag{72}$$

where:

$$\Delta\gamma = \tilde{\gamma} - \gamma_\xi \tag{73}$$

Here, the Lame constant μ has been replaced by the shear modulus G (see Eq. (64)).

Finally, the total shear stress in the phase transformation range ($\gamma \geqslant \gamma_\xi$) is equal to:

$$\begin{aligned}\tau^{\mathrm{p}} &= \tau_\xi + \Delta\tau^{\mathrm{p}1} + \Delta\tau^{\mathrm{p}2} \\ &= \tau_\xi + C_0\left[\Delta\gamma + \frac{h}{2}A(T)(\Delta\gamma)^2\right] + \frac{5}{2}G\eta_0\left[A(T)\frac{(\Delta\gamma)^2}{2} + (1+h)A^2(T)\frac{(\Delta\gamma)^3}{3} + (1+h)A^3(T)\frac{(\Delta\gamma)^4}{4}\right]\end{aligned} \tag{74}$$

where:

$$\tau_\xi = \tau_0 + C_0(\gamma_\xi - \gamma_0) \tag{75}$$

Here, the stress increment above the phase transformation threshold (γ_ξ, τ_ξ) is composed of three components (Fig. 10):

- linear hardening

$$\Delta\tau_{\mathrm{linear}} = C_0\Delta\gamma \tag{76}$$

- hardening due to interaction of dislocations with the martensite inclusions

$$\Delta\tau_{\mathrm{interaction}} = C_0\frac{h}{2}A(T)(\Delta\gamma)^2 \tag{77}$$

- hardening due to enhanced stiffness of two-phase continuum (M-T homogenization)

$$\Delta\tau_{\mathrm{MT}} = \frac{5}{2}G\eta_0\left[A(T)\frac{(\Delta\gamma)^2}{2} + (1+h)A^2(T)\frac{(\Delta\gamma)^3}{3} + (1+h)A^3(T)\frac{(\Delta\gamma)^4}{4}\right] \tag{78}$$

Assume the classical case of torsion where the shear strain γ is a function of the radius ρ:

$$\gamma = \vartheta\rho \tag{79}$$

and ϑ denotes the unit angle of twist. The torque can be obtained by integrating the shear stress multiplied by the current radius over the surface of the cross-section:

$$M_s = \iint_A \tau\rho \,\mathrm{d}A \tag{80}$$

Given all the components of the stress profile one obtains:

$$\begin{aligned}\frac{M_s}{2\pi} = &\int_0^{\rho_\mathrm{e}} G\vartheta\rho^3 \,\mathrm{d}\rho + \int_{\rho_\mathrm{e}}^{R} [\tau_0 + C_0(\vartheta\rho - \gamma_0)]\rho^2 \,\mathrm{d}\rho + \int_{\rho_\xi}^{R} C_0 \frac{h}{2} A(T)(\vartheta\rho - \gamma_\xi)^2\rho^2 \,\mathrm{d}\rho \\ &+ \int_{\rho_\xi}^{R} \frac{5}{2} G\eta_0 \left[A(T)\frac{(\vartheta\rho - \gamma_\xi)^2}{2} + (1+h)A^2(T)\frac{(\vartheta\rho - \gamma_\xi)^3}{3} + (1+h)A^3(T)\frac{(\vartheta\rho - \gamma_\xi)^4}{4}\right]\rho^2 \,\mathrm{d}\rho\end{aligned} \tag{81}$$

where ρ_e denotes the outer radius of the elastic zone and inner radius of the plastic zone, whereas, ρ_ξ denotes the outer radius of the plastic zone and the inner radius of the phase transformation zone. Both radii can be computed from the corresponding shear strain limits:

$$\rho_\mathrm{e} = \frac{\gamma_0}{\vartheta}; \quad \rho_\xi = \frac{\gamma_\xi}{\vartheta} \tag{82}$$

Assuming that the phase transformation process has already started from the outer radius of the circular cross-section ($M_s \geqslant M_\xi$), the torque is expressed by:

$$\begin{aligned}\frac{M_s}{2\pi} = &\frac{G\gamma_0^4}{4\vartheta^3} + \frac{\tau_0 - C_0\gamma_0}{3}(R^3 - \rho_\mathrm{e}^3) + \frac{C_0\vartheta}{4}(R^4 - \rho_\mathrm{e}^4) + \frac{A(T)}{2}\left[C_0 h + \frac{5G\eta_0}{2}\right]D_1 \\ &+ \frac{5}{2}G\eta_0 A^2(T)(1+h)\left[\frac{D_2}{3} + \frac{A(T)}{4}D_3\right]\end{aligned} \tag{83}$$

where:

$$D_1 = \vartheta^2\frac{R^5 - \rho_\xi^5}{5} - 2\vartheta\gamma_\xi\frac{R^4 - \rho_\xi^4}{4} + \gamma_\xi^2\frac{R^3 - \rho_\xi^3}{3} \tag{84}$$

$$D_2 = \frac{1}{3}\left[(\vartheta R - \gamma_\xi)^3 R^3 - (\vartheta\rho_\xi - \gamma_\xi)^3\rho_\xi^3\right] - \vartheta\left[\vartheta^2\frac{R^6 - \rho_\xi^6}{6} - 2\vartheta\gamma_\xi\frac{R^5 - \rho_\xi^5}{5} + \gamma_\xi^2\frac{R^4 - \rho_\xi^4}{4}\right] \tag{85}$$

$$\begin{aligned}D_3 = &\frac{1}{3}\left[(\vartheta R - \gamma_\xi)^4 R^3 - (\vartheta\rho_\xi - \gamma_\xi)^4\rho_\xi^3\right] - \frac{\vartheta}{3}\left[(\vartheta R - \gamma_\xi)^3 R^4 - (\vartheta\rho_\xi - \gamma_\xi)^3\rho_\xi^4\right] \\ &+ \vartheta^2\left[\vartheta^2\frac{R^7 - \rho_\xi^7}{7} - 2\vartheta\gamma_\xi\frac{R^6 - \rho_\xi^6}{6} + \gamma_\xi^2\frac{R^5 - \rho_\xi^5}{5}\right]\end{aligned} \tag{86}$$

Plotting the torque against the unit angle of twist $M_s = M_s(\vartheta)$ (Fig. 12) one has to specify the transition form purely elastic to the elastic–plastic response:

$$\bar{M}_s = \frac{\pi}{2}\tau_0 R^3 \tag{87}$$

as well as the transition from the elastic–plastic to the phase transformation regime:

$$M_\xi = \frac{\pi}{6}\left\{\tau_0 R^3(4 - \chi^3) + C_0 R^3\left[3\gamma_\xi(1 - \chi^4) - 4\gamma_0(1 - \chi^3)\right]\right\} \tag{88}$$

where:

$$\chi = \frac{\gamma_0}{\gamma_\xi} \tag{89}$$

The field of the residual stresses can be easily obtained by applying the following equations of elastic unloading:

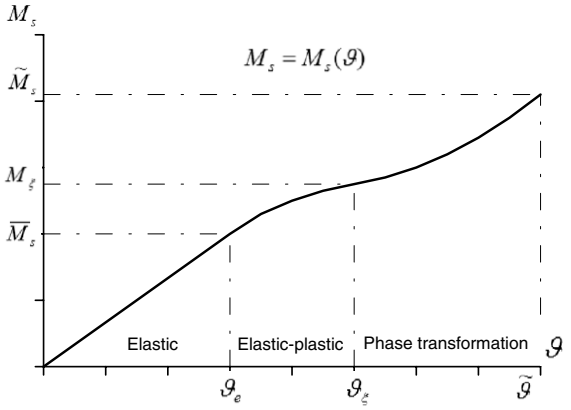

Fig. 12. Torque as a function of the unit angle of twist.

$$\tau^{\mathrm{r}} - \tau^{\mathrm{i}} = G(\gamma^{\mathrm{r}} - \gamma^{\mathrm{i}}) \tag{90}$$

$$M_{\mathrm{r}} = \iint_A \tau^{\mathrm{r}} \rho \, \mathrm{d}A = 0 \tag{91}$$

where $\gamma^{\mathrm{i}}, \tau^{\mathrm{i}}, \gamma^{\mathrm{r}}, \tau^{\mathrm{r}}, M_{\mathrm{r}}$ denote the initial shear strain and stress fields (before unloading), the residual shear strain and stress fields (after unloading) and the residual torque, respectively. Eq. (91) corresponds to the total unloading process.

5. Structural members with the functionally graded microstructure

Assume a structural member made of stainless steel (for instance grade 316L) subjected to torsion at low temperature, as shown in Fig. 13.

In order to obtain a functionally graded structure of the material the following condition has to be fulfilled:

$$M_s > M_\xi \tag{92}$$

which means that the phase transformation zone has started propagating towards the centre of the cross-section, as illustrated in Fig. 14.

Using the previously identified material properties of the grade 316L stainless steel at 77 K:

$$\gamma_0 = 0.0046; \quad \tau_0 = 363.7[\mathrm{MPa}]; \quad \gamma_\xi = 0.156; \quad \tau_\xi = 617.9[\mathrm{MPa}] \tag{93}$$

$$G = 79230.8[\mathrm{MPa}]; \quad C_0 = 1680[\mathrm{MPa}]; \quad h = 2.7; \quad A = 4.4; \quad \eta_0 = 0.0082 \tag{94}$$

one obtains the shear stress profile is shown in Fig. 15.

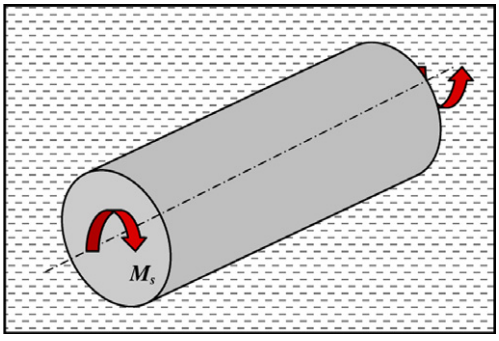

Fig. 13. Structural member subjected to torsion at low temperatures (liquid nitrogen or helium).

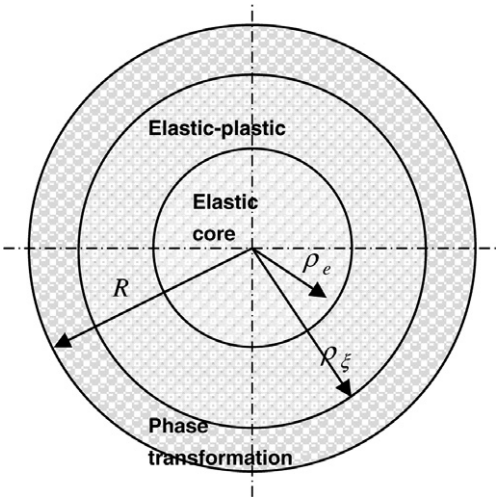

Fig. 14. Functionally graded structure of the structural member.

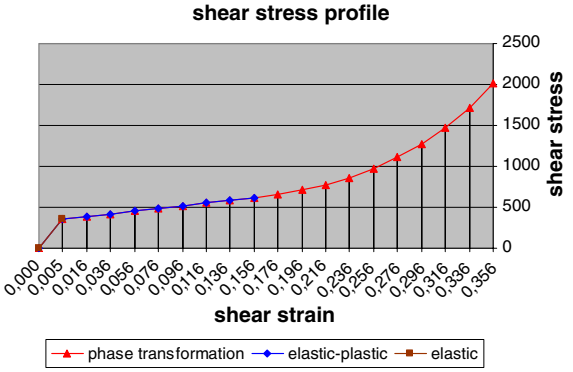

Fig. 15. Shear stress profile in the structural member subjected to elastic–plastic torsion.

Here, the shear stress is presented as a function of the shear strain $\tau = \tau(\gamma)$, however, by using the relation (79) it can easily be transformed to the function $\tau = \tau(\rho)$. In the present example the phase transformation limit ξ_L has been set – for the sake of simplicity – to 1. The profile of the volume fraction of martensite is shown in Fig. 16.

It is worth pointing out that the material structure is functionally graded in terms of the volume fraction of martensite starting from the radius ρ_ξ towards the outer radius of the structural member. This zone constitutes simultaneously a zone of substantial hardening of the material. All three components of the hardening induced by the $\gamma \rightarrow \alpha'$ phase transformation:

- basic linear hardening,
- hardening due to interaction of dislocations with the martensite inclusions,
- hardening reflected by the enhanced stiffness of two-phase continuum (Mori–Tanaka homogenization),

are plotted in Fig. 17. It is certainly worth emphasizing that the most pronounced contribution to the material hardening comes from the enhanced stiffness of the two-phase continuum due to the Mori–Tanaka homogenization (mixture of hard α' phase and soft γ phase). Thanks to the functionally graded material structure the outside surface of the structural member becomes much harder when compared to the soft elastic–plastic core. A micro-graph corresponding approximately to the functionally graded material structure

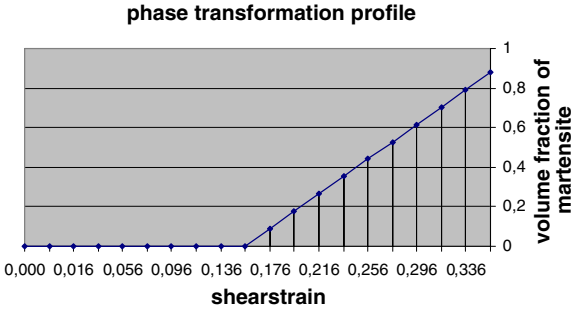

Fig. 16. Volume fraction of martensite against shear strain in the structural member (77 K).

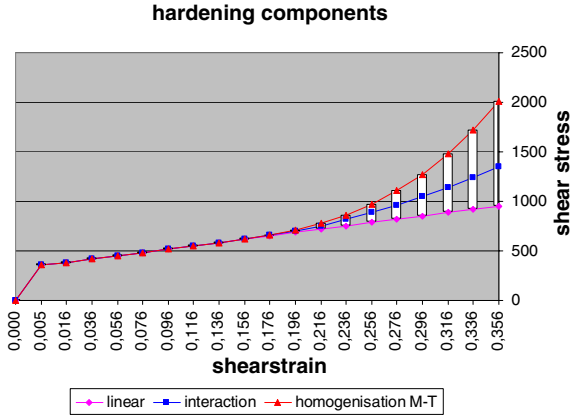

Fig. 17. Components of the strain hardening induced by the $\gamma \rightarrow \alpha'$ phase transformation.

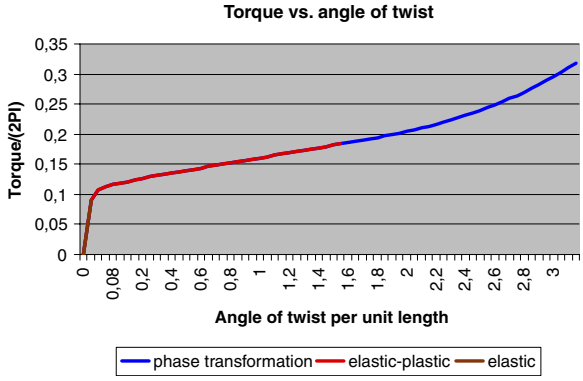

Fig. 18. Torque as a function of angle of twist per unit length.

is shown in Fig. 9. Finally, torque as a function of angle of twist per unit length has been plotted in Fig. 18 for the angle ranging from 0 to π. The radius of the structural member equal to 0.1 has been assumed in the numerical analysis.

6. Conclusions

In the present paper, a method of creating a functionally graded structural member by transforming its material at cryogenic temperatures has been shown. The technique is fairly simple and consists in imposing

on a stainless steel bar kinematically controlled torsion until the phase transformation threshold is reached and the material starts transforming itself close to the outside radius of the bar. The depth of the transformed zone is controlled by the angle of twist. In the transformed zone the face cubic centred (FCC) austenitic lattice is gradually replaced by the body cubic centred (BCC) martensitic structure of the material. The profile of the volume fraction of martensite in the transformed zone is linear and corresponds to the concept of functionally graded material (FGM). Thanks to the plastic strain induced phase transformation and the strain hardening the outside surface of the bar becomes much harder than the elastic–plastic core. A real gain in the overall stability of the bar under the axial compressive load and better protection of the outside surface against the mechanical damage are expected. The implications of the evolution of material structure for the stability of the structural member will be shown in a separate paper.

The constitutive model used to describe mathematically the plastic strain induced phase transformation at low temperatures involves strain hardening where two fundamental effects play an important role: interaction of dislocations with the martensite inclusions and increase in material tangent stiffness due to the mixture of harder martensite with softer austenite. The interaction of dislocations with the martensite inclusions is reflected by the hardening modulus that depends on the volume fraction of martensite. Here, a linear approximation, based on the micro-mechanics analysis, has been used. Evaluation of the resulting material tangent stiffness based on the classical homogenization scheme and taking into account the local tangent moduli of the components of two-phase continuum follows the concept by Hill, 1965. In the present paper, the Mori–Tanaka homogenisation scheme has been applied. Both effects contribute to strong nonlinear hardening as soon as the phase transformation process begins. The material model is suitable for a wide range of temperatures, however the best results are obtained at very low temperatures where the linearized kinetic law of phase transformation is valid. For the process of monotonic loading (torsion) the closed form solutions for the stress profile and torque are obtained.

Finally, it is worth pointing out that the proposed functionally graded structural members can be applied both at low and at higher temperatures since the plastic strain induced phase transformation occurring in metastable stainless steels (304L, 316L, etc.) at low temperatures transforms the material structure in an irreversible way.

Acknowledgements

The paper is written in memory of Professor Michał Życzkowski who passed away in 2006 leaving a great contribution to mechanics of materials and structures.

Grant of Polish Ministry of Science and Education: PB 4 T07A 027 30 (2006-2008) is gratefully acknowledged.

Also, I acknowledge the hospitality of IFMA, Clermont-Ferrand, where I have written part of this paper.

References

Aboudi, J., Pindera, M.J., Arnold, S.M., 1999. Higher-order theory for functionally graded materials. Composites B 30, 777–832.

Aboudi, J., Pindera, M.J., Arnold, S.M., 2003. Higher-order theory for periodic multiphase materials with inelastic phases. Int. J. Plast. 19, 805–847.

Alzina, A., Toussaint, E., Beakou, A., Skoczen, B., 2006. Multiscale modelling of thermal conductivity in composite materials for cryogenic structures. Composite Struct. 74 (2), 175–185.

Benveniste, Y., 1987. A new approach to the application of Mori–Tanaka's theory in composite materials. Mech. Mater. 6, 147–157.

Benvenuti, C., Circelli, N., Hauer, M., 1984. Niobium films for superconducting accelerating cavities. Appl. Phys. Lett. 45, 583–584.

Benvenuti, C., Chiggiato, P., Parrini, L., Russo, R., 1993. Reactive diffusion produced niobium nitride films for superconducting cavity applications. Nucl. Instrum. Meth. Phys. Res. A336, 16–22.

Benvenuti, C., Chiggiato, P., Escudeiro-Santana, A., Hedley, T., Mongelluzzo, A., Ruzinov, V., Wevers, I., 2001. Vacuum properties of TiZrV non-evaporable getter films for LHC vacuum system. Vacuum 60, 57–65.

Cherkaoui, M., Berveiller, M., Lemoine, X., 2000. Couplings between plasticity and martensitic phase transformation: overall behavior of polycrystalline TRIP steels. Int. J. Plast. 16, 1215–1241.

Dachowski, S., Boehm, M., 2004. Finite thermoplasticity with phase changes based on isomorphisms. Int. J. Plast. 20 (2), 323–334.

Diani, J.M., Parks, D.M., 1998. Effects of strain state on the kinetics of strain induced martensite in steels. J. Mech. Phys. Solids 46 (9), 1613–1635.

Doghri, I., Ouaar, A., 2003. Homogenization of two-phase elasto-plastic composite materials and structures: study of tangent operators, cyclic plasticity and numerical algorithms. Int. J. Solids Struct. 40 (7), 1681–1712.
Eshelby, J.D., 1957. The determination of the elastic field of an ellipsoidal inclusion, and related problems. Proc. R. Soc. Lond. Ser A 241, 376–396.
Fischer, F.D., 1997. Modeling and simulation. In: Berveiller, M., Fischer, F.D. (Eds.), Mechanics of Solids with Phase Changes, No. 368. Springer, Wien, New York, pp. 189–237.
Fischer, F.D., Oberaigner, E.R., Tanaka, K., Nishimura, F., 1998. Transformation induced plasticity revised an updated formulation. Int. J. Solids Struct. 35 (18), 2209–2227.
Fischer, F.D., Reisner, G., Werner, E., Tanaka, K., Cailletaud, G., Antretter, T., 2000. A new view on transformation induced plasticity (TRIP). Int. J. Plast. 16 (7–8), 723–748.
Garion, C., Skoczeń, B., 2002. Modeling of plastic strain induced martensitic transformation for cryogenic applications. J. Appl. Mech. 69 (6), 755–762.
Garion, C., Skoczeń, B., Sgobba, S., 2006. Constitutive modelling and identification of parameters of the plastic strain induced martensitic transformation in 316L stainless steel at cryogenic temperatures. Int. J. Plast. 22 (7), 1234–1264.
Goupee, A.J., Vel, S.S., 2006. Two-dimensional optimization of material composition of functionally graded materials using meshless analyses and a genetic algorithm. Comput. Methods Appl. Mech. Engrg. 195, 5926–5948.
Hashin, Z., Shtrikman, S., 1963. A variational approach to the theory of the elastic behaviour of multiphase materials. J. Mech. Phys. Solids 211, 127–140.
Hecker, S.S., Stout, M.G., Staudhammer, K.P., Smith, J.L., 1982. Effects of strain state and strain rate on deformation-induced transformation in 304 stainless steel: Part I. Magnetic measurements and mechanical behaviour. Metall. Trans. A 13A, 619–626.
Hershey, A.V., 1954. The elasticity of an isotropic aggregate of anisotropic cubic crystals. J. Appl. Mech. 21, 236–240.
Han, H.N., Lee, C.G., Oh, C.-S., Lee, T.-H., Kim, S.-J., 2004. A model for deformation behavior and mechanically induced martensitic transformation of metastable austenitic steel. Acta Mater. 52 (17), 5203–5214.
Hill, R., 1965. A self consistent mechanics of composite materials. J. Mech. Phys. Solids 13, 213–222.
Iwamoto, T., 2004. Multiscale computational simulation of deformation behavior of TRIP steel with growth of martensitic particles in unit cell by asymptotic homogenization method. Int. J. Plast. 20 (4–5), 841–869.
Kieback, B., Neubrand, A., Riedel, H., 2003. Processing techniques for functionally graded materials. Mater. Sci. Eng. A362, 81–105.
Koizumi, M., 1992. The concept of FGM. In: Proceedings of the Second International Symposium on the Functionally Graded Materials at the Third International Ceramic Science and Technology Congress, San Francisco, USA.
Koizumi, M., Niino, M., 1995. Overview of FGM research in Japan. MRS Bull. 20, 19–21.
Koizumi, M., 1997. FGM activities in Japan. Composites B 28B, 1–4.
Kordas, Z., Wróblewski, A., 1987. The problem of full plastification of circular cylinder with asymmetric nonhomogeneity. Rozp. Inz. 35 (2), 327–340.
Kordas, Z., Dollar, A., 1990. Non-homogeneous, circular thick-walled fully plasticized at failure cylinders under non-uniformly distributed pressure. Mech. Teor. Stos. 28 (1–2).
Kröner, E., 1958. Berechnung der elastischen Konstanten des Vielkristalls aus den Konstanten des Einkristalls. Z. Physik. 151, 504–518.
Levitas, V.I., Idesman, A.V., Olson, G.B., 1999. Continuum modeling of strain-induced martensitic transformation at shear band intersections. Acta Mater. 47 (1), 219–233.
Mori, T., Tanaka, K., 1973. Average stress in matrix and average elastic energy of materials with misfitting inclusions. Acta Metall. Mater. 21, 571–574.
Morris, J.W., Chan, J.W., Mei, Z., 1992. The influence of deformation-induced martensite on the cryogenic behavior of 300-series stainless steels. Cryogenics ICMC Suppl. 32, 78–85.
Narutani, T., Olson, G.B., Cohen, M., 1982. Constitutive flow relations for austenitic steels during strain-induced martensitic transformation. Journal de Physique, Colloque C4, supplement au N^o 12, Tome 43, 429–434.
Nemat-Nasser, S., 1999. Averaging theorems in finite deformation plasticity. Mech. Mater. 31, 493–523.
Nemat-Nasser, S., 2000. Multi-inclusion method for finite deformations: exact results and applications. Mater. Sci. Eng. A285, 239–245.
Olson, G.B., Cohen, M., 1975. Kinetics of strain-induced martensitic nucleation. Metall. Trans. 6A, 791–795.
Olszak, W., Urbanowski, W., 1955. Elastic–plastic thick-walled non-homogeneous cylinder subjected to internal pressure and longitudinal load. AMS 7 (3), 315–336, in Polish.
Olszak, W., Murzewski, J., 1957. Elastic–plastic bending of non-homogeneous orthotropic circular plates. AMS 9 (4), 467–485, 5, 605–629.
Olszak, W., Sawczuk, A., 1957. Problems of the limit analysis and design of non-homogeneous axially symmetric shells, 2nd CSRC, 249–256.
Paul, B., 1960. Prediction of elastic constants of multiphase materials. Trans. Metall. Soc. AIME, 36–41.
Pierard, O., Friebel, C., Doghri, I., 2004. Mean-field homogenization of multi-phase thermo-elastic composites: a general framework and its validation. Composites Sci. Technol. 64, 1587–1603.
Pierard, O., Doghri, I., 2006. An enhanced affine formulation and the corresponding numerical algorithms for the mean fields homogenization of elasto-viscoplastic composites. Int. J. Plast. 22 (1), 131–157.
Pindera, M.J., Dunn, P., 1997. Evaluation of the higher-order theory for functionally graded materials via the finite element method. Composites B 28B, 109–119.
Rooney, F., Ferrari, M., 2001. Tension, bending and flexure of functionally graded cylinders. Int. J. Solids Struct. 38, 413–421.
Sacchi, G., 1971. Limit analysis and design of structures having elements with random distribution of yield stresses, with associated and non-associated flow laws. Mec 6 (1), 65–68.

Smith, G.F., Spencer, A.J.M., 1970. A continuum theory of a plastic-rigid solid reinforced by two families of inextensible fibres. QJMAM 23 (4), 489–504.

Sofiyev, A.H., Schnack, E., 2004. The stability of functionally graded cylindrical shells under linearly increasing dynamic torsional load. Eng. Struct. 26, 1321–1331.

Stringfellow, R.G., Parks, D.M., Olson, G.B., 1992. Constitutive model for transformation plasticity accompanying strain-induced martensitic transformations in metastable austenitic steels. Acta Metall. 40 (7), 1703–1716.

Suzuki, K., Fukakura, J., Kashiwaya, H., 1988. Cryogenic fatigue properties of 304L and 316L stainless steels compared to mechanical strength and increasing magnetic permeability. Am. Soc. Testing Mater., 190–197.

Tarn, J.Q., 2001. Exact solutions for functionally graded anisotropic cylinders subjected to thermal and mechanical loads. Int. J. Solids Struct. 38, 8189–8206.

Tarn, J.Q., Wang, Y.M., 2001. Laminated composite tubes under extension, torsion, bending, shearing and pressuring: a state space approach. Int. J. Solids Struct. 38, 9053–9075.

Tomita, Y., Iwamoto, T., 2001. Computational prediction of deformation behavior of TRIP steels under cyclic loading. Int. J. Mech. Sci. 43 (9), 2017–2034.

Van Sciver, S.W., 1986. Helium Cryogenics. Plenum Press, New York.

Watanabe, Y., Sakai, H., 2003. Control of magnetic gradient in magnetically graded materials fabricated by martensitic transformation technique. Mater. Sci. Forum, 423–425, 435–440.

Wechsler, M.S., Lieberman, D.S., Read, T.A., 1953. On the theory of the formation of martensite. AIME Trans. J. Metals 197, 1503–1515.

Yang, Y.Y., 2000. Time-dependent stress analysis in functionally graded materials. Int. J. Solids Struct. 37, 7593–7608.

Życzkowski, M., 1957a. The limit load of a thick-walled tube in a general circularly symmetrical case. AMS 8 (2), 155–179, 9th ICAM 1956, 8, 1957, 129–139.

Życzkowski, M., 1957b. Limit state of non-homogeneous rotating circular disks. 9th ICAM 1956 6, 351–360.

Życzkowski, M., 1981. Combined loadings in the theory of plasticity. PWN – Polish Scientific Publishers, Warsaw, Poland.